A&A 642, A56 (2020)
https://doi.org/10.1051/0004-6361/202037942

Astronomy & Astrophysics

The *Gaia*-ESO Survey: A new diagnostic for accretion and outflow activity in the young cluster NGC 2264⋆

R. Bonito[1], L. Prisinzano[1], L. Venuti[2,1], F. Damiani[1], G. Micela[1], G. Sacco[3], G. Traven[4], K. Biazzo[5], L. Sbordone[6], T. Masseron[7,8], T. Zwitter[9], A. Gonneau[10], A. Bayo[11,12], V. Roccatagliata[13,3,14], S. Randich[3], J. S. Vink[15], P. Jofre[16], E. Flaccomio[1], L. Magrini[3], G. Carraro[17], L. Morbidelli[3], A. Frasca[5], L. Monaco[18], E. Rigliaco[19], C. Worley[10], A. Hourihane[10], G. Gilmore[10], E. Franciosini[3], J. Lewis[10,⋆⋆], and S. Koposov[10]

[1] INAF – Osservatorio Astronomico di Palermo, P.zza del Parlamento 1, 90134 Palermo, Italy
e-mail: rosaria.bonito@inaf.it
[2] NASA Ames Research Center, Moffett Blvd, Mountain View, CA 94035, USA
[3] INAF – Osservatorio Astrofisico di Arcetri, Largo E. Fermi, 5, 50125 Firenze, Italy
[4] Lund Observatory, Department of Astronomy and Theoretical Physics, Box 43, 221 00 Lund, Sweden
[5] INAF – Osservatorio Astrofisico di Catania, Catania, Italy
[6] ESO – European Southern Observatory, Alonso de Cordova 3107, Vitacura, Santiago, Chile
[7] Instituto de Astrofisica de Canarias, 38205 La Laguna, Tenerife, Spain
[8] Departamento de Astrofisica, Universidad de La Laguna, 38206 La Laguna, Tenerife, Spain
[9] Faculty of Mathematics and Physics, University of Ljubljana, Jadranska 19, 1000 Ljubljana, Slovenia
[10] Institute of Astronomy, University of Cambridge, Madingley Road, Cambridge CB3 0HA, UK
[11] Instituto de Fisica y Astronomia, Universidad de Valparaiso, Valparaiso, Chile
[12] Nucleo Milenio Formacion Planetaria – NPF, Universidad de Valparaiso, Valparaiso, Chile
[13] Dipartimento di Fisica Enrico Fermi, Universita di Pisa, Largo Pontecorvo 3, 56127 Pisa, Italy
[14] INFN, Sezione di Pisa, Largo Pontecorvo 3, 56127 Pisa, Italy
[15] Armagh Observatory, and Planetarium, BT61 9DG Armagh, College Hill, UK
[16] The Astronomy Nucleus at Universidad Diego Portales, Santiago, Chile
[17] Dipartimento di Fisica e Astronomia, Universita di Padova, Vicolo Osservatorio 3, 35122 Padova, Italy
[18] Departamento de Ciencias Fisicas, Universidad Andres Bello, Fernandez Concha 700, Las Condes, Santiago, Chile
[19] INAF – Osservatorio Astronomico di Padova, Padova, Italy

Received 12 March 2020 / Accepted 16 July 2020

ABSTRACT

Context. NGC 2264 is a young cluster whose accretion properties can be investigated in detail by taking advantage of the FLAMES data in the context of the *Gaia*-ESO Survey. In fact, the analysis of the Hα emission line profile can provide us with information about the accretion and ejection activity of young stars. However, a strong nebular emission that contributes to the Hα emission can alter the profiles, with consequences for their physical interpretation.
Aims. Our study is aimed at investigating the accretion and ejection properties of NGC 2264 by applying a proper treatment of the sky contribution to the Hα and forbidden emission lines (FELs; [SII] and [NII] doublets).
Methods. We developed a tool, the OHαNA-method, to handle the strong nebular contribution and spectra with spurious profiles of the Hα and FELs, namely altered Hα profiles or absorption features artificially created where emission lines (FELs) are expected. We derived the quantitative measurements of relevant parameters to describe the accretion and ejection processes in young members of NGC 2264, focusing on reliable quantities derived from the width of the lines, which is relatively unaffected by the nebular emission, unlike the intensity peak, which can be altered significantly.
Results. We derive the quantitative measurements related to the Hα emission line and discuss the comparison between the original and sky-subtracted spectra. We thus reveal possible profile alterations with consequences for their physical interpretation. Furthermore, we show the analysis of the variability for multi-epoch observations, also deriving the velocity of the infalling and outflowing plasma from the wings of the broad Hα emission line (in accreting stars). We also explore the mass accretion rate versus full width at zero intensity of the Hα line, namely $\dot{M}$ versus FWZI(Hα), a correlation based on the width of the emission line, which is expected to be more robust with respect to any measurement derived from the peak (e.g., H$\alpha_{10\%}$) and possibly altered by the nebular contribution.
Conclusions. We are able to ascertain that more than 20% of the confirmed accretors, which have already been identified in NGC 2264, are affected by the alteration of their line profiles due to the contribution of the nebular emission. Therefore, this is an important issue to consider when investigating accretion and ejection processes in young stellar clusters. While a small fraction of spectra can be unequivocally classified as either unaffected by nebular emission or dominated by nebular emission, the majority (>90%) represent intermediate cases whose spectral features have to be investigated in detail to derive reliable measurements of the relevant parameters and their physical implications.

Key words. stars: formation – stars: pre-main sequence – accretion, accretion disks – stars: winds, outflows – line: profiles – open clusters and associations: individual: NGC 2264

⋆ Full Tables 1, A.1, and A.2 are only available at the CDS via anonymous ftp to cdsarc.u-strasbg.fr (130.79.128.5) or via http://cdsarc.u-strasbg.fr/viz-bin/cat/J/A+A/642/A56
⋆⋆ Jim Lewis passed away before the paper was completed, but he gave a significant contribution to the GES analysis that was fundamental for this paper.

1. Introduction

Accretion and ejection processes in young stellar objects (YSOs) are phenomena that characterize the star formation process itself. These opposing processes are intimately correlated, as stellar jets in YSOs are observed only when there is any accretion of material onto the forming stars from the environment or the disk. Mass accretion onto the stellar surface is present during the early-stages of YSOs, from class 0 and class I protostars (Lada 1987) that are deeply embedded into the surrounding material to class II (or classical T Tauri stars, CTTSs), where the circumstellar disk is still active and material from the disk accretes onto the central star through the magnetic field lines (Koenigl 1991). Emission in a wide range of wavelengths is produced by shocks formed at the interaction front between supersonic jets and the ambient medium as well as at the stellar surface due to infalling material. This has also been explored using numerical models and laboratory experiments (Bonito et al. 2011, 2014; Albertazzi et al. 2014; Revet et al. 2017). In the optical band, the Hα line is a well-known proxy for the accretion and outflow activity (Reipurth et al. 1996), whereas the forbidden emission lines (FELs) can identify an ongoing outflow process (see e.g., Rigliaco et al. 2009 for σ Ori).

These YSOs are usually found within the original molecular cloud close to the HII emission triggered by the ionizing radiation from nearby massive stars. This leads to a contribution to the emission lines in the stellar spectra that should be properly removed when YSO properties have to be deduced through a spectral analysis. We present the study of the mass accretion and outflow properties in members of the young cluster NGC 2264 that takes advantage of the analysis of the Hα 6563 Å emission line profile and the forbidden emission lines, namely, the [SII] 6717/6731 Å and [NII] 6548.05/6583.45 Å doublets. We developed a method to investigate the family of spectra of stars contaminated by a dominant nebular contribution to the emission that we define as "Objects with Hα emission and strong Nebular contribution to signature of Accretion/outflow activity", or "OHαNA". These objects can be found in several clusters, many of which are targets of the *Gaia*-ESO Survey (GES; Gilmore et al. 2012; Randich et al. 2013), such as NGC 2264 (Jackson et al. 2016; Venuti et al. 2018), NGC 6530 (Prisinzano et al. 2007, 2019), and NGC 6611 (Bonito et al. 2013).

The new methodology here presented, the OHαNA-method, is applied to NGC 2264. NGC 2264 is a young stellar cluster with an age of ≈3 Myr located at a distance of ≈760 pc (Dahm et al. 2008; see also an estimation of the distance of 719 pc by Maiz Apellaniz 2019 using *Gaia* DR2 data). It has been studied in several wavelength-bands, ranging from infrared (IR) to X-ray, thus allowing robust criteria for cluster membership. In the context of a multi-wavelength project, NGC 2264 has been chosen as a target for observations with several instruments as part of the campaign of the Coordinated Synoptic Investigation of NGC 2264 (CSI 2264; Cody et al. 2014). The NGC 2264 cluster has been already investigated in GES by Traven et al. (2015), who cataloged the Hα emission stars, Jackson et al. (2016), who discussed the membership of the cluster, Bouvier et al. (2016), who presented a Li study, and Venuti et al. (2018), who demonstrated the presence of multiple substructures and subpopulations, with multiple star formation events having occurred in this star-forming region.

Here, we present the analysis of the full width at zero intensity (FWZI) of the Hα line and develop a method that can provide us with quantitative measurements related to the accretion process for those cases where the nebular contribution is strong, entailing the consequence that the equivalent width (EW) and H$\alpha_{10\%}$ (i.e., the width of the Hα line at 10% of its peak) estimations are not reliable. More specifically, we use our approach to identify potentially contaminated cases (where nebular subtraction is not satisfactory) and then we base our analysis only on the FWZI measurements which are free from nebular component contamination. In this paper, we also present and discuss an automated procedure developed to address this issue.

The FWZI(Hα) can be considered a reliable estimation of the Hα emission line width, as it is typically much larger than the FWZI(Hα) associated to the pure sky spectra (FWZI(H$\alpha_{\rm sky}$) ≈ 3 Å, see an estimation of the nebular FWZI in Bonito et al. 2013). A discrimination between active and inert disks is made possible by the investigation of the FWZI(Hα) and, in general, of the Hα line profile. Indeed, an active disk will show a broad Hα emission line due to the accretion and outflow activity, while an inert disk will correspond to a narrow Hα profile that is usually indistinguishable with respect to the nebular contribution. Besides the analysis of the Hα emission line, the FELs provide us with information on the outflow process at work in the star and, therefore, they can also be useful to discriminate between active and inert disks. This is helpful in the investigation of the different timescales involved in the processes of accretion and disk dissipation.

The paper is organized as follows. In Sect. 2, we present the data used and our analysis. In Sect. 3, we show our results concerning the accretion and ejection processes in YSOs, including the physical interpretation of the line profiles and their variability. We discuss our results and we draw our conclusions in Sect. 4. The *OHαNA − method* tool is presented in Appendix A.

2. Data set and analysis

2.1. GES data

We use the GES (Gilmore et al. 2012; Randich et al. 2013) observations of NGC 2264, performed with the spectrograph GIRAFFE at the Very Large Telescope multi-object optical facility FLAMES (using the HR15 setup, covering a wavelength range of 6444−6816 Å; Pasquini et al. 2002) between December 2011 and January 2013. Target selection follows the guidelines adopted by GES for young open clusters (Randich et al. 2018). In this paper, we use the fifth internal data release (GES iDR5), which is the most recent release available at the time of the analysis.

For the purposes of this work, we use both the reduced spectra of GES iDR5, where the sky-subtraction has been performed using the standard pipeline, and the spectra prior to sky-subtraction (see details in Sect. 2.2). We analyzed both the sky-subtracted and the original (non-sky-subtracted) spectra because one of the aims of this work is to compare the profiles of the Hα and FELs in the different spectra to highlight any discrepancy attributed to the sky subtraction. Furthermore, we used the non-co-added spectra to also investigate the variability of the accretion and ejection processes. We analyzed a total of 7535 spectra: 2095 are pure sky spectra, while 5440 are spectra of stellar targets (all GES targets in NGC 2264, independently with respect to any previous membership classification), corresponding to 1875 different objects, some with multiple spectra (60% with 20 observations, considering also archival data; 25% with just one spectrum; 15% with 2 to 6 spectra), useful for the variability analysis. Here, 87% (4811) of the total number of stellar spectra have a signal-to-noise ratio (S/N) higher than 10, while ≈50% (2649) have $S/N > 40$ (see Table 1).

2.2. Data analysis

Sky-subtraction could lead to the formation of spurious line profiles. The extreme case of over-subtraction of the sky can in fact result in the formation of spurious absorption lines where only emission lines (FELs like [SII] and [NII]) are expected (Appenzeller et al. 1984). This can have implications for the interpretation of the outflow activity or for the age estimation and membership. Therefore, the sky subtraction can lead to, as a consequence, the misinterpretation of the physical properties of the stars based on the emission line profile analysis (Reipurth et al. 1996). It is worth noting that it is not possible to solve the issue by improving the S/N or by using higher resolution instruments, as this is a problem related to the physical presence of the nebular emission. Furthermore, the nebular contribution is spatially variable (Damiani et al. 2016) and cannot be easily measured independently. The data reduction includes the step involving sky-subtraction. This nebular contribution to the emission of the main lines characterizing the accretion and outflow properties of young members is a significant issue for this cluster (Lanzafame et al. 2015). Therefore, it is important to include a proper treatment of the sky-subtraction.

In this context, the investigation of the FELs or of the spurious absorption lines can be useful both for the physics (outflow activity) of the cluster members and as a proxy for a successful sky-subtraction. In particular, we developed a tool (see Appendix A) to flag the spectra which show spurious absorption which would provide the warning information that in those cases, the use of the original (non-sky-subtracted) spectra and the FWZI(Hα) measurements is highly recommended. Using the FWZI approach, we can perform quantitative measurements of the plasma velocity due to infalling material from the disk on the stellar surface (when accretion process is at work) or due to material ejected in the surrounding medium (when outflow process occurs) by investigating the wings in the red and blue part of the Hα line profile, respectively.

As the variability of the nebular contribution is expected on longer time scales (Damiani et al. 2016) than those considered here (see Sect. 3.2), any relative variation can be derived from the original non-sky-subtracted spectrum. We note that the flagged spectra not only indicate an over-subtracted sky contribution (leading to a spurious-absorption FEL) but, more importantly, prevent us from misinterpreting the physical properties of the system under analysis. Based on the presence of spurious absorption lines, we define the extreme ("good" and "bad") cases (see Appendix A and Tables A.1 and A.2). Briefly, the good cases are spectra with FWZI(Hα) > 14 Å that do not show spurious absorption lines due to an over-subtraction of the nebular contribution (no flag, as defined in Appendix A) and among them, we define the objects with Hα line in emission as "confident accretors". Bad cases are spectra whose diagnostic is seriously affected by nebular emission, with the consequence that no accurate measurement is possible, with FWZI(Hα) < 3 Å, and we define these objects "non-accretors". Intermediate cases are spectra that should be checked case by case and we define them "candidate accretors" if the Hα line is in emission and their FWZI(Hα) > 4 Å (as in Prisinzano et al. 2019), and they do not show spurious absorption lines due to an over-subtraction of the sky (no flag, see discussion in Appendix). We will refer to "confirmed accretors" for the accretors investigated in previous works, also using different techniques (e.g., Venuti et al. 2018).

3. Results

We analyzed the profile of the Hα line and the [SII] and [NII] doublets FELs that are the emission lines relevant for the study of accretion and ejection processes (see Table 1).

The *OHαNA – method* tool that we developed allows us to flag spurious absorption lines (see Appendix A). Briefly, we selected a 50 Å-wide region of the original spectrum centered on the line of interest. Then we normalized the spectrum to the continuum, isolating the expected emission line. In Table 2, we show the classification of good and bad cases (the good cases also being confident accretors when their Hα line is in emission, a condition that holds for ≈90% of the total good cases), and some information on intermediate cases (in particular those with flag for each FEL and OHαNA with no flag), as discussed in detail in Appendix A.

3.1. Line profiles and spurious lines

In Fig. 1, we compare the original spectrum (lilac dashed line) with the sky-subtracted spectrum (black line) for three cases: (1) a good case, as defined in Appendix A (i.e., without any flag from the tool and a large Hα emission line, FWZI > 14 Å, see Appendix A); (2) an intermediate case, with a flag from the tool and broad Hα line profile (FWZI > 4 Å); (3) a case flagged from the tool and with a narrow Hα line profile (FWZI < 4 Å).

Among the good cases, the member 06404114+0933578 (left panel in Fig. 1), shows the largest value of FWZI(Hα) (≈20 Å) and it is a class II accreting star (CSIMon-000469 in Venuti et al. 2018; therefore this is a confirmed accretor). This object shows two almost indistinguishable curves (compare lilac-dashed curve and black curve). Therefore, the sky contribution is small and the parameters related to the Hα measurements can all be considered reliable, including those derived from the value of the peak of the Hα line profile.

The intermediate case, the flagged member 06392550+0931394 (middle panel in Fig. 1) is a class II accreting star (CSIMon-006491 in Venuti et al. 2018; therefore we consider this as a confirmed accretor) showing a broad Hα line profile with a double peak in the sky-subtracted spectrum (black line). The comparison between the original spectrum (lilac dashed line) and the sky-subtracted spectrum (black line) in Fig. 1, reveals the spurious absorption FELs [NII] 6548/6583 Å around the Hα emission and the altered Hα line profile (without the double peak in the original spectrum). This is possibly due to a shift in the median sky used for the subtraction of the nebular contribution (see also sky spectrum in Fig. 2 in cyan). However, the wings of the Hα emission line are wide and almost identical both in the original and in the sky-subtracted spectra. Therefore, any measurement related to the width of the emission line, such as the FWZI and the velocity of infalling and ejected plasma in similar cases, are reliable also in the sky-subtracted spectra. On the contrary, caution should be taken when considering parameters derived from the peak of the emission line, such as the H$\alpha_{10\%}$ (and therefore $\dot{M}$ when the Natta et al. 2004 relation is used to derive this parameter) and EW(Hα), as well as for any physical deduction based on the interpretation of the emission line profiles (see Reipurth et al. 1996 and Bonito et al. 2013), as these could be strongly altered by the nebular contribution.

The flagged case, member 06395328+0949458 (right panel in Fig. 1) is a class III star that is, nonetheless, accreting (as discussed in Venuti et al. 2018, where this object is also indicated

Table 1. Cname, spectrum used for the measurements, object name, signal-to-noise ratio, FWZI(Hα) in Å, and velocities of the wings (blue and red part of the profile) of the Hα line in km s^{-1} for all the objects analyzed here.

Cname	MANYSPEC.Nspec	OBJECT	S/N	FWZI(Hα)	Vel(blue)	Vel(red)
06392396+0942016	C20121024-00047-st.124	8541-M	28	3.60	−18	146
06392408+0938088	C20121025-00041-st.126	8967-M	8	2.85	−27	103
06392497+0933151	C20121025-00041-st.113	10959-M	7	2.15	−30	69
06392506+0942515	C20121024-00047-st.123	8162-M	14	2.70	−41	82
06392535+0943147	C20121024-00047-st.122	7991-M	19	2.25	−53	50

Notes. The information presented in this table refers to all the GES targets, independently with respect to previous membership selections and their nature. The cases of interest for this paper are those with Hα line in emission, but we also report the values for cases with Hα line in absorption. Caution should be used when considering the values presented in this table for parameters related to accretion process when the Hα line is in absorption – see values of Hα 10% width in the electronic version of this table. These parameters have been derived from the non-sky-subtracted spectra. The complete version of this table is available at the CDS and includes more parameters: the coordinates; the values of Hα 10% width and the mass accretion rate (both the value from the Natta et al. 2004 relation and the new value from Eq. (1)) that have been derived from the non-sky-subtracted spectra (these parameters can be altered by the nebular emission as discussed in the main text); the extremes of the [SII] and [NII] doublets calculated by the tool and derived from the sky-subtracted spectra that give an indication of possible spurious absorption lines due to an over-subtraction of the nebular contribution. All the parameters have been derived in this work. Here, the information on the first five objects are reported as an example.

Table 2. Classification of spectra of all the targets as in Appendix A.

TYPE	FLAG	FWZI(Hα)	N. SPECTRA (N. DIFFERENT OBJECTS)
Good	N	>14 Å	218 (62)
Bad	Y (for each FEL)	<3 Å	56 (55)
Intermediate with flag for each FEL	Y (for each FEL)	>3 Å	73 (70), 2 confirmed accretors
Intermediate OHαNA with no flag	N	(4−14) Å	139 (53)

Notes. All the other cases are intermediate cases to be investigated in more detail. Among the good cases, the spectra showing Hα line in emission (≈90% of the total) are confident accretors. The intermediate OHαNA with no flag in this table are candidate accretors with also $S/N > 40$ and H$\alpha_{10\%} > 200$ km s^{-1} (as in Natta et al. 2004): by a visual inspection case-by-case, ≈90% of these spectra show altered profiles (from the comparison between original and sky-subtracted spectra). A case-by-case investigation of OHαNA objects and their variability is recommended, as described in the main text.

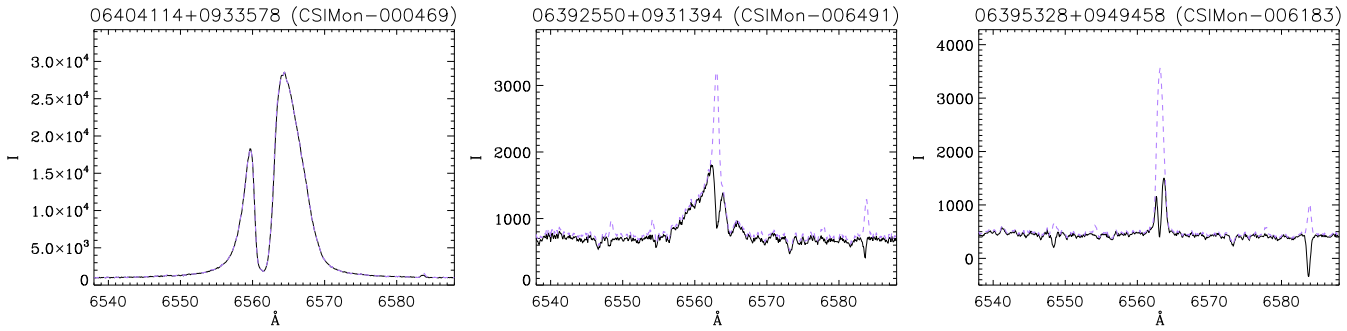

Fig. 1. Original (lilac dashed line) and sky-subtracted (black line) spectra for three cases: good case without a flag from the tool (*left panel*); intermediate case, with a flag from the tool and broad Hα line profile (*middle panel*); a case with a flag from the tool and narrow Hα line profile (*right panel*).

as CSIMon-006183), which shows a narrow Hα profile and a double peaked feature that could have been altered due to an over-subtraction of the sky. Nevertheless, even in these cases of narrow lines where the nebular contribution can be the dominant one, while the H$\alpha_{10\%}$ and EW(Hα) measurements cannot be performed in a proper way, the FWZI parameter is still reliable.

Figure 3 summarizes the information presented in Tables 1, 2, A.1, and A.2. The good and bad cases defined represent a small fraction of the total spectra, while the most interesting cases are the intermediate ones. Therefore, we decided to be conservative in their definition and to be more restrictive in the definition of the extreme cases (good and bad), that are here defined as confident accretors when their Hα line is in emission (≈90% of the total good cases) and as non-accretors. As an example, the no-flag member discussed above has a FWZI(Hα) ≈ 20 Å, the flagged wide member FWZI(Hα) is ≈8 Å, while the flagged narrow member FWZI(Hα) is ≈3.7 Å.

It is worth noting that OHαNA cases can be found also among objects which do not show spurious FELs in absorption due to an over-subtraction of the nebular contribution. Analyzing the OHαNA not flagged by the automated tool (i.e., the objects without spurious absorption features, but showing an altered Hα emission profile, and that can be considered accretors, as per the definition in Sect. 2.2), the comparison between the

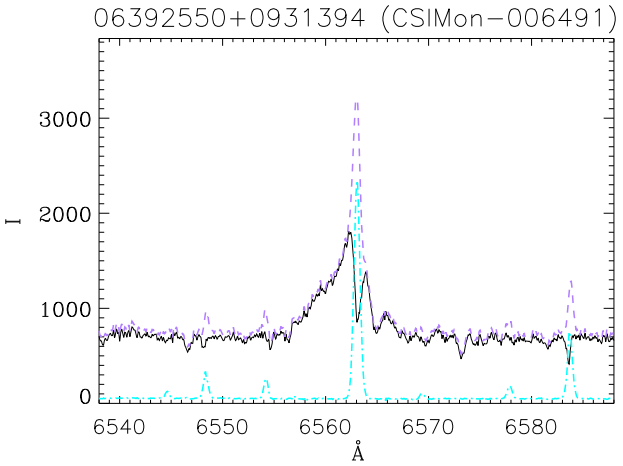

Fig. 2. Range of the spectrum of the object 06392550+0931394 (same object as that shown in Fig. 1, middle panel) around the Hα line, including the [NII] doublet. The original spectrum is shown in lilac dashed, the sky-subtracted spectrum in black, and the nebular contribution used for the sky subtraction is in cyan dashed-dotted lines.

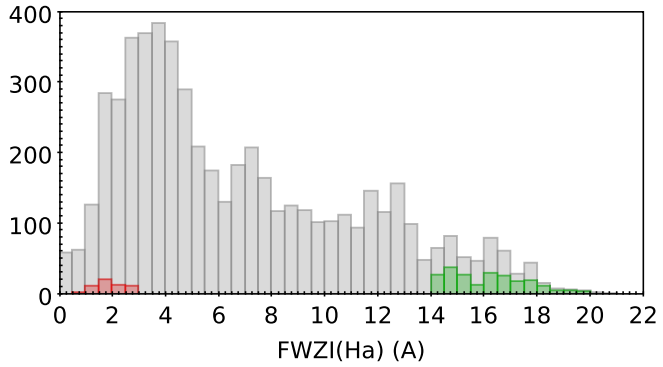

Fig. 3. Histogram of all the analyzed stellar spectra (in gray) as a function of the FWZI(Hα). The good cases are highlighted in green, the bad spectra in red.

original and the sky-subtracted spectra reveals that the profiles and peaks of the lines can be very different. This can have significant consequences on the measurements of the H$\alpha_{10\%}$ and EW(Hα). As an example, the member 06410194+0950038, classified as a class II accretor by Venuti et al. (2018) (therefore we consider this object as a confirmed accretor, and it is also indicated in Venuti et al. 2018 as CSIMon-000331) is shown in Fig. 4.

For the [SII] doublet, we derive that 2760/5440[1] spectra (more than 50%) have the 6717 Å line as a spurious absorption line, 1111/5440 (more than 20%) have both the lines of the [SII] doublet in absorption. Among the 187 confirmed accretors in NGC 2264 in Venuti et al. (2018) (see their Table B.1), our tool identified more than 20% of objects with flag (spurious lines) listed in Table 3: 38 with flag for the [SII] doublet; 4 with flag for the [NII] doublet; 2 with flag for all FELs[2].

In Fig. 5, the spatial distribution of all the targets discussed here is shown, with the confirmed accretors (identified by Venuti et al. 2018) highlighted as blue empty squares, with

[1] These numbers refer to the total spectra analyzed, excluding the pure sky spectra.

[2] As some objects are observed several times, the condition to have flag for all FELs should hold for at least one spectrum of these objects.

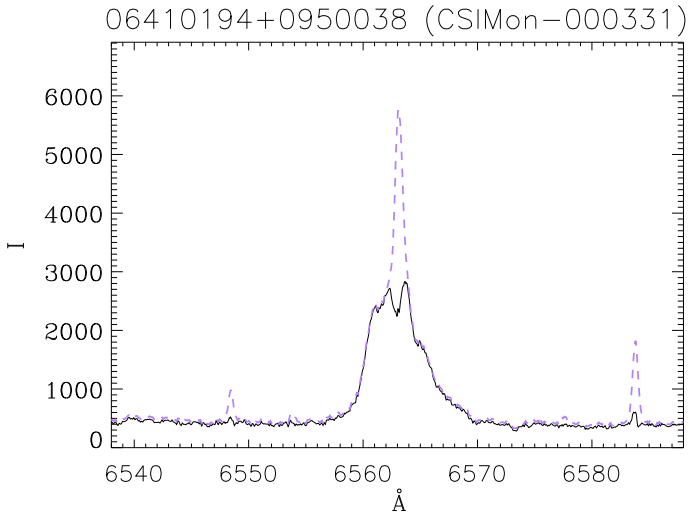

Fig. 4. Range of the spectrum around the Hα line including also the [NII] doublet for a non-flagged OHαNA case. The original spectrum is shown in lilac dashed, the sky-subtracted spectrum in black.

the good and bad cases highlighted as green and red dots, respectively. The confirmed accretors are found mostly concentrated in the central part as well as the good cases. Many confirmed accretors have been identified as good cases, as expected, but some accretors are among the intermediate cases to be further investigated, as highlighted by the new diagnostic presented here. The good and bad cases generally represent a small fraction of the total spectra, the fraction being even lower if limited to the confirmed members of NGC 2264 (see also Table 2).

3.2. Line profiles and their variability

Here, we derived and analyzed the line profiles, their physical interpretation (see Reipurth et al. 1996 and Bonito et al. 2013), their variability, and the values of the plasma velocity corresponding to the wings width and due to the motion of the plasma in infall and outflow. We discuss this analysis for selected members, representative of the good (06404114+0933578), the bad (06402778+0925193, defined as a bad case for one of its spectra), the accreting non-flagged OHαNA (06410194+0950038) members, and two intermediate cases (flagged for both FELs doublets of [SII] and [NII], but with a broad Hα emission line), that are also confirmed accretors (06401111+0921272 and 06404136+0954138; see Table 3).

The good case (member 06404114+0933578) shows almost identical profiles in the original and in the sky-subtracted spectra (as also shown in Fig. 1, left panel). The line profile is asymmetric and shows two well defined peaks, with a second emission peak whose intensity is greater than half of the main peak and is located blue-ward of the main peak. Therefore, following the classification of Reipurth et al. (1996), this is a type II-B profile. Following Kurosawa et al. (2006), the type II-B corresponds to medium-to-high inclinations and to fast wind acceleration. The FWZI(Hα) is large (19.95 Å), greater than the typical pure nebular contribution, due to the accretion and ejection processes at work for this star (in fact, this object has been identified as a young class II accretor by Venuti et al. 2018) and, therefore, to the motion of infalling and outflowing plasma. The values of the plasma velocity derived from the width of the wings corresponds to ≈ -440 and ≈ 470 km s^{-1}, and H$\alpha_{10\%}$ $\approx$ 570 km s^{-1} (consistent with the value reported by Venuti et al. 2018).

Table 3. Confirmed accretors with flag.

CNAME	FLAG	CLASS
06392550+0931394	SII	II
06393398+0949208	SII	–
06393939+0945215	SII	II
06394147+0946196	SII	–
06395328+0949458	SII	III
06395795+0941046	SII	II
06400215+0945143	SII	III
06400553+0922261	SII	II
06400600+0949426	SII	II
06401418+0934284	SII	II
06401780+0925478	SII	II
06402150+0906031	SII	II
06403652+0950456	SII	II
06403698+0939098	SII	–
06403746+0955212	SII	III
06403912+0950586	SII	II
06404132+0951023	SII	II
06404185+0951445	SII	II
06404601+0917582	SII	–
06405059+0954573	SII	–
06405364+0933247	SII	II
06405426+0949203	SII	II
06405518+0950498	SII	III
06405572+0951138	SII	II
06405883+0939187	SII	II
06410712+0912383	SII	II
06411292+0905257	SII	II
06411600+0916351	SII	II
06412402+1014321	SII	–
06412419+0948309	SII	II
06412562+0934430	SII	II
06413729+0945066	SII	II
06414188+0919282	SII	II
06415307+0958034	SII	–
06415493+0942527	SII	–
06405295+0926256	NII	II
06404940+0952540	SII OR NII	II
06401111+0921272	SII AND NII	–
06404136+0954138	SII AND NII	II

Notes. These confirmed accretors (see Venuti et al. 2018) show spurious [SII] doublet (FLAG = SII) or spurious [NII] doublet (FLAG = NII) in absorption or both (FLAG = SII AND NII, if in the same spectrum; FLAG = SII OR NII, if different spectra) in at least one spectrum, therefore are flagged by our automated tool. Their class as derived by Venuti et al. (2018) is also indicated in the last column.

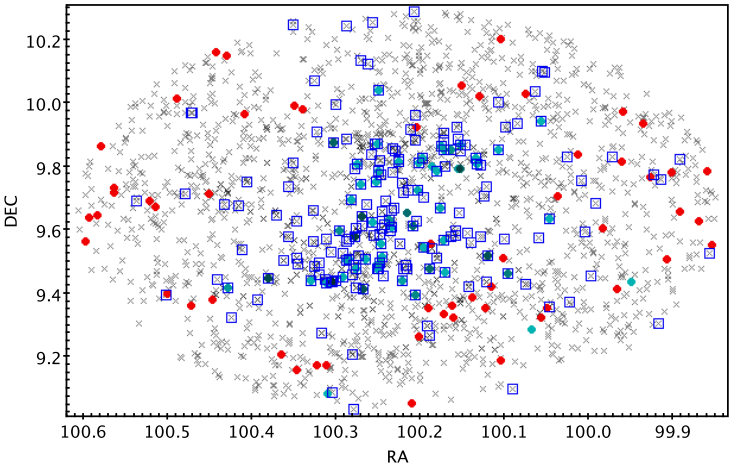

Fig. 5. Spatial distribution of all the targets (gray crosses) investigated here: blue empty squares are the confirmed accretors, while the green and red dots are the good and bad cases, respectively.

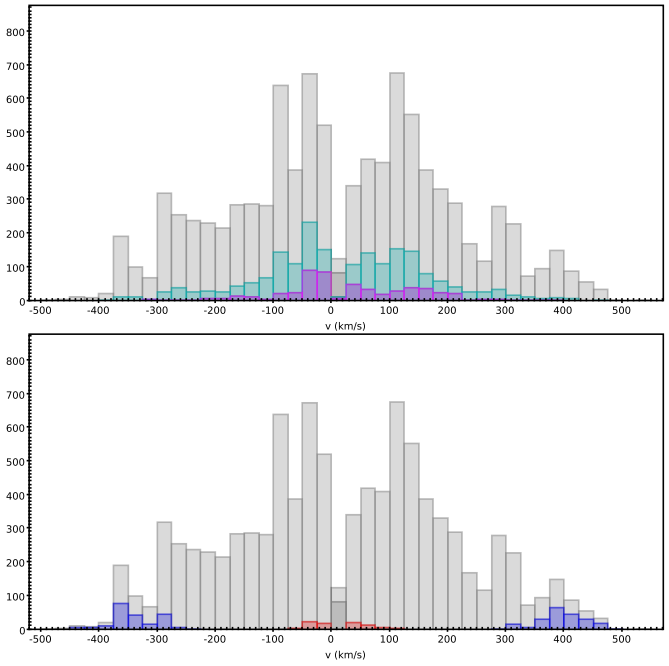

Fig. 6. Histograms as a function of the velocity derived from the wings of the Hα line for the spectra with $S/N > 10$. *Upper panel*: flagged spectra with spurious absorption doublets are highlighted in light blue for [SII] and in magenta for [NII]. *Lower panel*: good (blue) and bad (red) cases are highlighted.

In Fig. 6, we show the histograms of all the spectra with $S/N > 10$ as a function of the velocities derived from the blue- and red-shifted wings of the Hα line, with the spectra flagged for the spurious absorption FELs highlighted (upper panel: light blue for [SII] and magenta for [NII]) and the good and bad cases in blue and red, respectively (lower panel).

From this figure, it is evident that there are more spectra that have been flagged corresponding to a lower velocity, but also many spectra with large plasma velocities (corresponding to wide lines and therefore to possible accretors) are affected, mostly the intermediate cases with plasma velocities ranging between 100−300 km s^{-1}. Furthermore, the number of spectra flagged for [SII] spurious absorption is much higher than the analogous case of [NII] doublet, thus suggesting a stronger diagnostic power of the [SII] doublet. Figure 6 again shows that the intermediate cases are the most numerous, with the good and bad cases amounting to only a fraction of all spectra, corresponding to the highest (300−400 km s^{-1}) and lowest (<100 km s^{-1}) plasma velocity values, as expected.

For the bad case (member 06402778+0925193), the comparison between the original and the sky-subtracted spectrum reveals the modification of the Hα (and also of the [NII]) line profiles as an effect of the nebular contribution considered. The type profile is I (typical of pure nebular contribution) and it is narrow, with FWZI(Hα) $\approx$ 2.35 Å, that is, within the

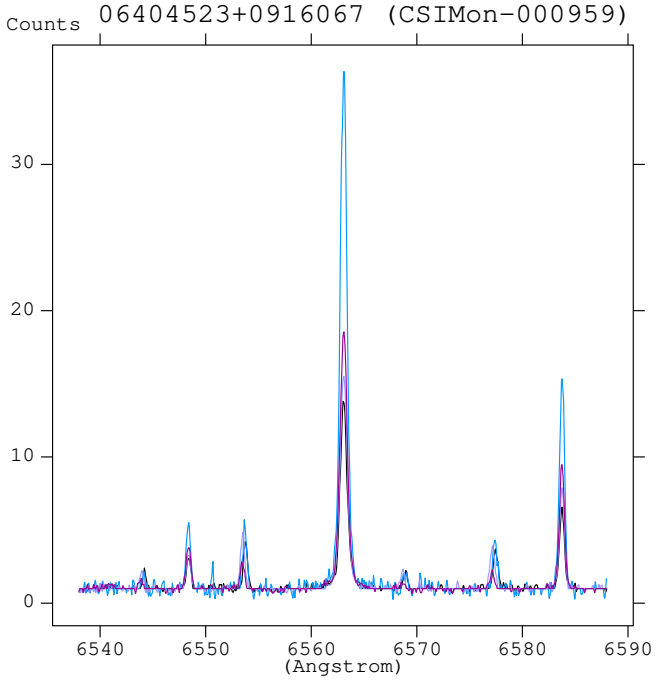

Fig. 7. Variability of the spectrum near the Hα emission line of the OHαNA not-flagged class II accretor 06404523+0916067 for the original spectra with FWZI greater than pure nebular contribution: different colours correspond to spectra collected in different observations of the same object.

characteristic sky width. In fact, this object has been classified as a bad spectrum and it is not an accretor.

The OHαNA not-flagged case (the class II confirmed accretor 06410194+0950038) shows an altered Hα emission line profile due to the effect of the sky subtraction, with evident reduction of the peak intensity (Fig. 4) when the original and the sky-subtracted spectrum are compared. To explore the variability, as this object has been observed in a single spectrum, here we discuss an OHαNA not-flagged case with multiple observations (even if there is low S/N), namely, the class II accretor 06404523+0916067. For this object, 20 different spectra were acquired and we derived a variability of the Hα line profile, which shows type I, IV B, or multi-peaks profiles. It is worth noting that the original spectra show variable intensity of the emission line (see the sample of spectra associated to this object that shows FWZI larger that the pure nebular contribution in Fig. 7), even for spectra whose Hα line profile type is I in all cases, while the profile type varies in the sky-subtracted spectra, showing also multi-peak features. The width of the emission line is in general small, with FWZI(Hα) $\approx$ 2.1−4.2 Å, and velocity of the wings ranges between $\approx -30-107$ km s^{-1}.

Among the intermediate cases, there are two confirmed accretors with spurious absorption for each FELs (flag; see last two cases in Table 3): 06401111+0921272 and 06404136+0954138 (CSIMon-001287 and CSIMon-001099 in Venuti et al. 2018, respectively), both observed in 20 different spectra (therefore a variability study can be performed), with intermediate and high S/N, respectively. The width of the Hα emission line (FWZI) is large and ranges between 9−14 Å and 6−14 Å for the two objects. The velocity derived from the wings is $\approx -300-350$ km s^{-1} and that derived from the total width is $\approx$400−640 km s^{-1} and 260−620 km s^{-1}, revealing the presence of plasma in motion due to the accretion and ejection processes. The profiles show asymmetry and multiple features. Comparing the original and the sky-subtracted spectra, the wings of the lines are almost identical in all the spectra, even if the central nebular contribution can alter the profiles (see Bonito et al. 2013). These objects are confirmed accretors with broad Hα emission and, therefore, we expected that outside the 3 Å central region (where the nebular contribution to the emission is dominant), the profiles would not be influenced by the contribution of the sky or by its subtraction. In fact, the wings are the most interesting regions of the Hα emission profile when it comes to providing physical information on the accretion and ejection processes and the plasma velocity. We derived that both the intensity and the profile types vary in significant ways (see Fig. 8).

Costigan et al. (2014) monitored the variability of the Hα profiles in 15 T Tauri and Herbig Ae stars, collecting data with a very close temporal coverage ($\approx$20 exposures in 1 hour) with respect to the time-scales investigated here (two consecutive exposures for the object shown in the upper panel of Fig. 8 are collected every $\approx$1 day while the total time is $\approx$3 months). The authors found common small changes (on the time-scales of days) and uncommon large changes in the Hα profiles of a few stars (on the time-scales of minutes). We found in the case shown in Fig. 8 a similarly large variability, which involves all the main parts of the profile, the blue- and red-wing as well as the central part, on longer time-scales. Therefore, the large changes associated to rapid events in Costigan et al. (2014) are also present in NGC 2264 and associated to longer time-scales (of course, we cannot exclude that the event is rapid also in NGC 2264 but we did not monitor it at the close temporal coverage available to Costigan et al. 2014). It is worth noting that the time-scales involved are different, therefore, we focus only on the profile variability considering its morphology. Furthermore, in our spectra the sky subtraction can be an issue, and we consider parameters derived from the non-sky-subtracted spectra. Therefore, we cannot compare the values of the same parameters in general. To quantify the changes, Costigan et al. (2014) considered the variations in EW and H$\alpha_{10\%}$. While Costigan et al. (2014) performed tests on the sky subtraction around Hα and concluded that this cannot be the cause of the variation of the rapid events, for NGC 2264, we demonstrated that the nebular contribution prevented us from trusting the measurements of these parameters in some cases. We can, instead, quantify the variability in term of FWZI for the two cases explored in Fig. 8: we derive an average of 11.5 Å, minimum of 8.8 Å, maximum of 14.1 Å, and standard deviation of 1.7 for 06401111+0921272, and an average of 10.8 Å, minimum of 5.7 Å, maximum of 13.6 Å, and standard deviation of 2.4 for 06404136+0954138.

4. Discussion and conclusions

In this paper, we present the analysis of the spectral data derived in the context of the *Gaia*-ESO Survey in NGC 2264, focusing on the accretion and ejection processes in young cluster members. The relevant emission lines in the optical band that allow us to investigate in detail the infalling and outflowing plasma are the Hα and the forbidden emission lines (FELs), namely, the [NII] and [SII] doublets. The contribution of the nebular emission is strong in these lines, thus making the sky-subtraction an issue for the young stellar members of clusters like NGC 2264.

To handle this problem, we developed a tool, the *OHαNA – method*, to flag the affected spectra (for which an over-subtraction of the nebular emission can lead to spurious absorption features). As the nebular contribution to the emission is narrow and almost centered on the Hα line, any measurement

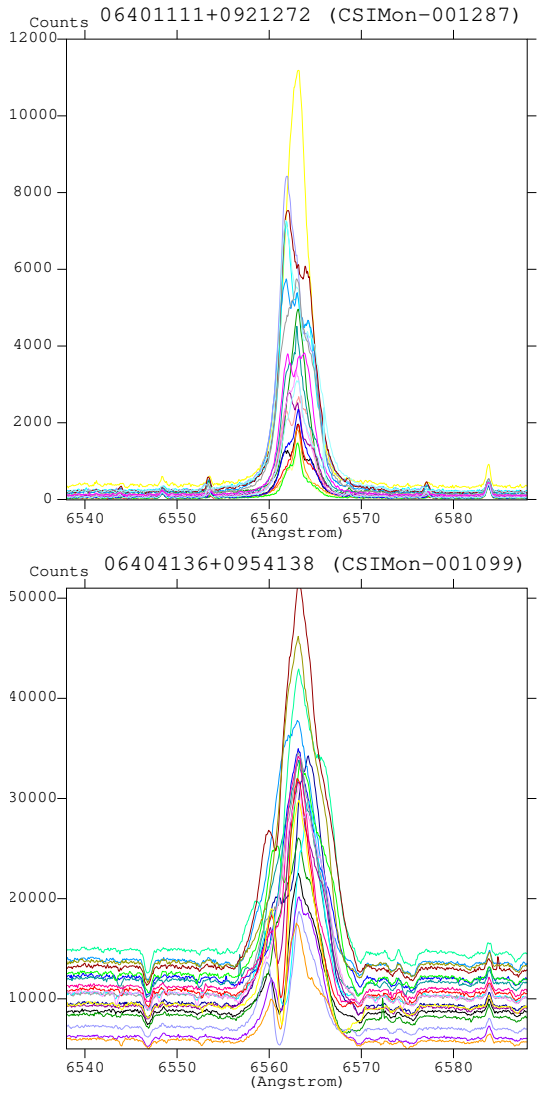

Fig. 8. Variability of the spectrum near the Hα emission line of the intermediate accretor 06401111+0921272 (*upper panel*) and of the class II accretor 06404136+0954138 (*lower panel*) for all the 20 original spectra collected for each of these stars. We note that to avoid confusion, the spectra are not continuum-normalized and, thus, the continua are different.

derived from the peak of the Hα, as the H$\alpha_{10\%}$ (and, consequently, the $\dot{M}$ derived from this value using the empirical relation described in Natta et al. 2004) are not reliable because they can be strongly affected by the dominant nebular emission. However, the wings of the Hα line, that reflect the presence of infalling and outflowing material in young stars with active accretion and ejection processes, whose motion causes a broad Hα emission profile, are not affected by the narrow sky contribution that alters the central peak of the line. Therefore, we compared the stellar contribution to the pure nebular contribution (typically as narrow as a few Å) and we suggest that we can trust any measurement derived from the width of the line, but not from its central peak. Here we propose using the quantitative information that can be obtained by the FWZI of the Hα emission line, which is a reliable parameter, being derived by the width of the line not affected by the nebular contribution as its peak.

As any measurement derived from the width of the emission line is more robust with respect to that derived from the peak, which may possibly be altered by the nebular contribution, it can be helpful to search for a correlation between $\dot{M}$ and FWZI in an analogous way as the empirical relation derived by Natta et al. (2004), using the H$\alpha_{10\%}$. We explored the $\dot{M}$ vs. FWZI correlation[3] in the good cases with Hα line in emission given that these objects are confident accretors. We focused on the spectra with high S/N (>40) and H$\alpha_{10\%}$ > 200 km s^{-1}, as was also assumed by Natta et al. (2004). For these spectra, we verified that the sky-subtracted and the original spectra are identical or very similar, so we can derive reliable measurements from the peak, as the H$\alpha_{10\%}$. In total, these are 37 objects with a total of 121 spectra. The best-fit relation found with our analysis between these two quantities is:

$$\log(\dot{M}_{\rm bestfit}) = -14.64(\pm0.47) + 0.39(\pm0.03) \times {\rm FWZI(H}\alpha). \quad (1)$$

and it is shown in Fig. 9.

Barentsen et al. (2013) derived mass accretion rate estimations using Bayesian inference applied to photometric survey data for pre-main sequence stars in NGC 2264. The discrimination between accretors and non-accretors in that paper is based on the accretion luminosity with respect to the chromospheric saturation limit (therefore a different criterion with respect to the one presented here) and an empirical relationship (Barentsen et al. 2013, Eq. (22)). That relationship shows a strong scatter due to emission (which is not due to accretion) which could also be related to the nebular contribution discussed here. These authors applied their method to 587 objects selected in NGC 2264 and derived that the accretion fraction is ≈20% (115 objects in Barentsen et al. 2013), but this estimate does not account for very low levels of accretion nor the variability in the accretion process. This value of frequency is in good agreement with clusters of similar age (Fedele et al. 2010). Comparing the mass accretion rate derived by Barentsen et al. (2013) and this paper, they found $\log(\dot{M}) = (-10.7 - -6.4)\ M_\odot\,{\rm yr}^{-1}$, with a median $\log(\dot{M}) = -8.4\ M_\odot\,{\rm yr}^{-1}$, and we derive from the new relation: $\log(\dot{M}) = (-9.0 - -6.9)\ M_\odot\,{\rm yr}^{-1}$, with a median $\log(\dot{M}) = -8.0\ M_\odot\,{\rm yr}^{-1}$, considering the good cases defined as confident accretors focusing on the spectra with high S/N (>40) and H$\alpha_{10\%}$ > 200 km s^{-1} (those used to derive the relation in Eq. (1)).

This preliminary investigation on the $\dot{M}$ vs. FWZI correlation seems to be promising and this is to be the subject of a forthcoming paper (Bonito et al., in prep.), which will include a comparison of several clusters affected by the nebular contamination (NGC 2264, but also e.g., NGC 6530 and NGC 6611).

Our results also suggest that the original (non-sky-subtracted) spectra should be analyzed and compared with the sky-subtracted ones in order to derive the correct line profiles, from which proper physical interpretation related to the infalling and outflowing plasma, their velocity and variability, can be inferred. Therefore, we were able to investigate the accretors (active disks) in NGC 2264, also describing their variability and the velocity of the material accreting onto the star and the influence of the motion on the emission line profiles. Our tool for flagging altered spectra allowed us to identify "good" and "bad" cases, with regard to the strong nebular emission which affects the line profile and whose over-subtraction can lead to spurious absorption lines. A comparison between the original and the sky-subtracted spectra is required in particular for those cases, indicated as OHαNA, whose Hα line is altered by the nebular emission and active accretion process, but without a spurious absorption feature that can reveal them.

[3] Deriving the $\dot{M}$ using the Natta et al. (2004) relation.

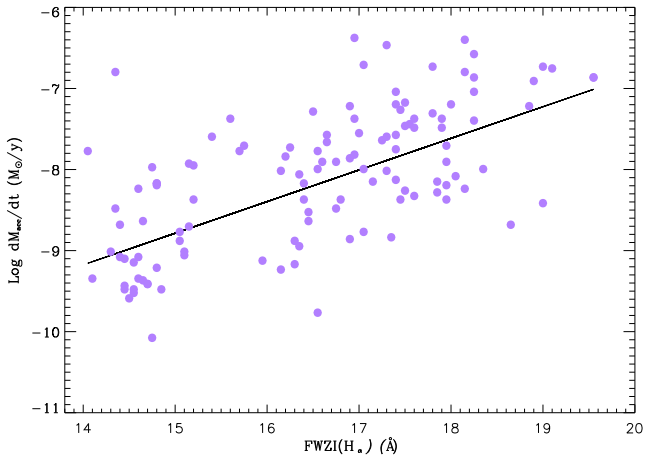

Fig. 9. log($\dot{M}$) derived from the H$\alpha_{10\%}$ following the Natta et al. (2004) as a function of the FWZI for the good cases with Hα line in emission, the confident accretors, with high S/N (>40), and H$\alpha_{10\%}$ > 200 km s^{-1}, whose spectra are not altered by the nebular contribution and therefore allow us to derive reliable measurements from their peak. The data of the good cases are shown as lilac dots and the best-fit line is superimposed.

More than 50% of the analyzed spectra (excluding the pure nebular spectra) show one spurious absorption [SII] line, while more that 20% have both [SII] lines of the doublet altered by the nebular over-subtraction, with consequences for the correct interpretation of the physical processes at work in those objects. In particular, more than 20% of the accretors identified by Venuti et al. (2018) in NGC 2264 were flagged using our tool for the presence of spurious absorption lines. In fact, in Venuti et al. (2018), other photometric information was also used to deal with possibly affected objects like these and to avoid any misinterpretation in their analysis.

Multi-epoch observations allow us to also investigate the variability of the profiles and the related accretion and ejection processes. In fact, it is well-known that these processes are variable and this is reflected in the emission lines intensity, their profile, and the derived velocities. Young stellar objects are also characterized by photometric variability that is caused by several processes (mass accretion, presence of warps in envelopes and disks, the creation of new knots in stellar jets, stellar rotation, star-spots, magnetic cycles, and flares), as also discussed in, for example, Venuti et al. (2015), Stauffer et al. (2014), and Bonito et al. (2018) (for the future Vera C. Rubin Observatory Legacy Survey of Space and Time, LSST).

In conclusion, we take advantage of an important issue, namely, the alteration of emission lines due to the strong nebular contribution to the emission of relevant lines for the study of accretion and ejection processes, converting its potential negative effect into the opportunity to flag the affected spectra with a method based on an automated tool developed by our group. This can hold consequences for the analysis of young stellar clusters and their accretors members, as in the case of NGC 2264. The issue we investigate here and the solution we propose can be of interest for future surveys of stellar clusters and star-forming regions as well as for new-generation instruments. For instance, the WEAVE multi-object survey spectrograph and the 4-metre Multi-Object Spectroscopic Telescope (4MOST) will allow for observations of stellar clusters and star-forming regions. For the regions affected by intense nebular contribution, the young members with accretion and ejection processes can be investigated using the methods discussed in this paper.

Acknowledgements. Based on data products from observations made with ESO Telescopes at the La Silla Paranal Observatory under program IDs 188.B-3002, 193.B.0936, and 197.B-1074. These data products have been processed by the Cambridge Astronomy Survey Unit (CASU) at the Institute of Astronomy, University of Cambridge, and by the FLAMES/UVES reduction team at INAF/Osservatorio Astrofisico di Arcetri. These data have been obtained from the *Gaia*-ESO Survey Data Archive, prepared and hosted by the WideField Astronomy Unit, Institute for Astronomy, University of Edinburgh, which is funded by the UK Science and Technology Facilities Council. We thank the anonymous referee for their useful comments and suggestions. R.B. would like to thank Dr. Serena Benatti (INAF – Osservatorio Astronomico di Palermo) and Dr. Costanza Argiroffi (University of Palermo – Dept. Of Physics and Chemistry) for their kind help. R. B., L. P., and F. D. acknowledge modest financial contribution from the agreement ASI-INAF n.2017-14.H.O. R. B. acknowledges financial support by PRIN-INAF 2013 Disks, jets and the dawn of planets (PI: Nisini). A. G. acknowledges support from the European Union FP7 programme through ERC grant number 32036 and from the UK space agency. T. Z. acknowledges the financial support from the Slovenian Research Agency (research core funding No. P1-0188). T. M. acknowledges support provided by the Spanish Ministry of Economy and Competitiveness (MINECO) under grant AYA-2017-88254-P. E. R. is supported by the European Union's Horizon 2020 research and innovation programme under the Marie Skłodowska-Curie grant agreement No 664931. L. V. acknowledges support by an appointment to the NASA Postdoctoral Program at the NASA Ames Research Center, administered by Universities Space Research Association under contract with NASA.

References

Albertazzi, B., Ciardi, A., Nakatsutsumi, M., et al. 2014, Science, 346, 325
Appenzeller, I., Oestreicher, R., & Jankovics, I. 1984, A&A, 141, 108
Barentsen, G., Vink, J. S., Drew, J. E., & Sale, S. E. 2013, MNRAS, 429, 1981
Bonito, R., Orlando, S., Miceli, M., et al. 2011, ApJ, 737, 54
Bonito, R., Prisinzano, L., Guarcello, M. G., & Micela, G. 2013, A&A, 556, A108
Bonito, R., Orlando, S., Argiroffi, M., Miceli, M., et al. 2014, ApJ, 795, 34
Bonito, R., Hartigan, P., Venuti, L., et al. 2018, ArXiv eprints [arXiv:1812.03135]
Bouvier, J., lanzafame, A., Venuti, L., et al. 2016, A&A, 590, A78
Cody, A. M., Stauffer, J., Baglin, A., et al. 2014, AJ, 147, 82
Costigan, G., Vink, J. S., Scholz, A., Ray, T., & Testi, L. 2014, MNRAS, 440, 3444
Dahm, S. E. 2008, in Handbook of Star Forming Regions, Volume I: The Northern Sky ASP Monograph Publications, ed. B. Reipurth, 4, 966
Damiani, F., Bonito, R., , Magrini, L. et al. 2016, A&A, 591, A74
Fedele, D., van den Ancker, M. E., Henning, Th., et al. 2010, A&A, 510, A72
Gilmore, G., Randich, S., Asplund, M., et al. 2012, Messenger, 147, 25
Jackson, R. J., Jeffries, R. D., Randich, S., et al. 2016, A&A, 586, A52
Koenigl, A. 1991, ApJ, 370, L39
Kurosawa, R., Harries, T. J., & Symington, N. H. 2006, MNRAS, 370, 580
Lada, C. J. 1987, IAU Symp., 115, 1
Lanzafame, A. C., Frasca, A., Damiani, F., et al. 2015, A&A, 576, A80
Maiz Apellaniz, J. 2019, A&A, 630, A119
Natta, A., Testi, L., Muzerolle, J., et al. 2004, A&A, 424, 603
Pasquini, L., Avila, G., Blecha, A., et al. 2002, Messenger, 110, 1
Prisinzano, L., Damiani, F., Micela, G., & Pillitteri, I. 2007, A&A, 462, 123
Prisinzano, L., Damiani, F., Kalari, V., et al. 2019, A&A, 623, A159
Randich, S., Gilmore, G., & the Gaia-ESO Consortium 2013, Messenger, 154, 47
Randich, S., Tognelli, E., Jackson, R., et al. 2018, A&A, 612, A99
Reipurth, B., Pedrosa, A., & Lago, M. T. V. T. 1996, A&AS, 120, 229
Revet, G., Chen, S. N., Bonito, R., et al. 2017, Sci. Adv., 3, 11
Rigliaco, E., Natta, A., Randich, S., & Sacco, G. 2009, A&A, 495, L13
Smiljanic, R., Korn, A. J., et al. 2014, A&A, 570, A122
Stauffer, J., Cody, A. M., , Baglin, A., et al. 2014, AJ, 147, 83
Traven, G., Zwitter, T., Van Eck, S., et al. 2015, A&A, 581, A52
Venuti, L., Bouvier, J., , Irwin, J. et al. 2015, A&A, 581, A66
Venuti, L., Prisinzano, L., Sacco, G. G., et al. 2018, A&A, 609, A10

Appendix A: Flag for spurious forbidden emission lines (FELs) in absorption: an automated tool

We address the problem of OHαNA objects (see the definition in Sect. 1) by proposing a solution based on an automated tool developed at INAF-OAPa. The automated approach will allow us to keep our analysis as homogeneous as possible.

As a first step of our automated tool to flag the spurious absorption features in the [NII] 6548.05/6583.45 Å and [SII] 6717/6731 Å doublets, we select a region 50 Å wide of the spectrum centered on the [SII] doublet in the range 6700–6750 Å and centered on the Hα line in the range 6538–6588 Å for the [NII] doublet (see the example in first and second panels of Fig. A.1).

Then we continuum-normalize the spectrum using the IRAF task *continuum*, selecting as output the data minus any rejected point replaced by the fit[4]. An example of the output of this step is shown in third panel of Fig. A.1. The last step allows us to isolate the emission lines by performing the ratio between the spectrum and the normalized spectrum (see fourth panel in Fig. A.1). We can easily flag the spectra whose FELs are in absorption and therefore are spurious (see an example in Fig. A.2)[5]. We define a flag for those cases where more than half of the points are in absorption.

By comparing the original non-sky-subtracted spectra with the sky-subtracted spectra we can derive the nebular contribution assumed. Such a comparison reveals how good the analysis of the sky-subtracted spectra can be and which parameters can be considered reliable and which should be used at least with caution. As OHαNA cases can be found also among objects not showing spurious FELs in absorption caused by over-subtraction of the nebular contribution, it is necessary to compare the sky-subtracted spectra with the original non-sky-subtracted spectra. In fact, we suggest using the original spectra, which are very useful for investigating any alteration on the line profiles.

We define the extreme cases as: 1) spectra that do not show spurious absorption features due to an over-subtraction of the nebular contribution and have a large Hα line (see below the value of FWZI), which we define as "good"; 2) spectra altered in a significant way that the information derived from the lines (especially from the peak of the emission lines) are not reliable, which we define as "bad". We developed an automated tool to define "good" or "bad" cases by considering the absence (no-flag) or presence (flag) of spurious lines due to an over-subtraction of the nebular contribution in concurrence with the information on the width of the Hα emission line (more specifically, the measurement of its FWZI). In particular: 1) the good cases are defined as non-flagged[6] spectra with FWZI(Hα) > 14 Å[7] and we define these as "confident accretors" when their Hα line is in emission (this condition holds for ≈90% of the total good cases); 2) the bad cases are defined as flagged spectra[8] with FWZI(Hα) < 3 Å[9]and are likely non-accretors. Considering all the spectra (including pure sky spectra and repeated spectra used for variability study), the bad cases are: 153/7535; these numbers are reduced to 56/5440 when considering repeated

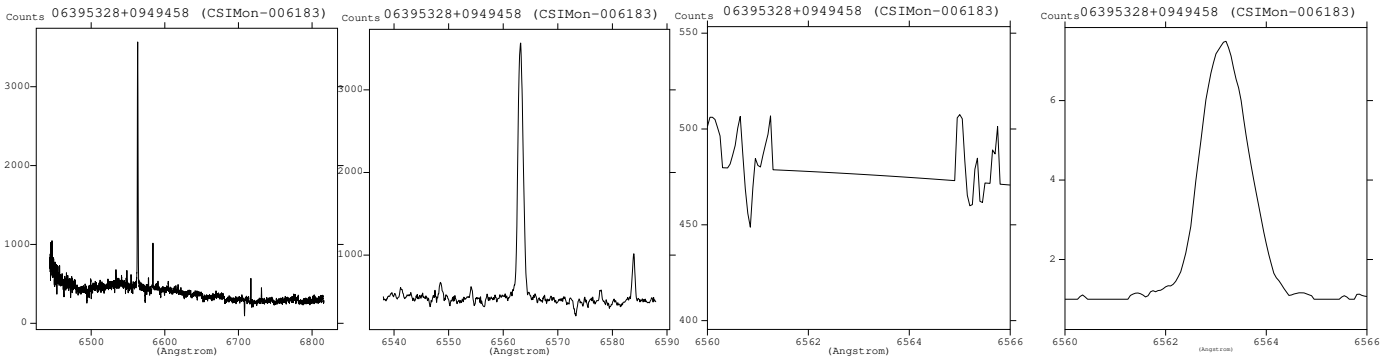

Fig. A.1. Steps to isolate the line of interest: (1) total spectrum (*first panel*); (2) zoomed spectrum (*second panel*); (3) spectrum with suppression of the line (*third panel*); (4) isolated line (*fourth panel*).

[4] NOAO: https://www.stsci.edu/documents/dhb/web/c03_stsdas.fm5.html#932455

[5] For the [SII] doublet, we consider both the 6717 Å and the 6731 Å line for the flag as the near Ca I line could be in absorption due to physical reasons.

[6] This condition should hold for any of the FELs, both [SII] and [NII] doublets.

[7] We considered an histogram to define the bulk of the FWZI(Hα) derived for accreting stars in NGC 2264 and obtained a value of ≈12 Å, but in Prisinzano et al. (2007) for NGC 6530 the authors define WTTS a star with a 13.5 Å. In order to be more conservative for the intermediate cases, and therefore more restrictive with the definition of "good" cases, we use the higher value of 14 Å.

[8] This condition should hold for all of the FELs, both [SII] and [NII] doublets.

[9] This value has been derived from Bonito et al. (2013) for the case of NGC 6611 for the pure sky spectra. Also for NGC 2264 we found that the bulk of spectra shows FWZI(Hα) ≈ 3 Å; only a few cases of pure sky spectra with a broad Hα line have been also found and they will be discussed in more detail in Bonito et al. (in prep.). The pure sky spectra with FWZI(Hα) > 3 Å are ≈10%, this number reducing to 5% considering FWZI(Hα) > 4 Å. As previously explained, to be more conservative, we should use the lower value in order to be more restrictive in the definition of "bad" cases. Therefore we decide to use the lower value of 3 Å.

spectra but not the pure sky spectra, corresponding to 55 different objects. Analogously, the good cases are: 218/7535 or 218/5440[10], corresponding to 62 different objects. The extreme bad cases make up, therefore, ∼1% of the total, while the good cases are ≈4% of the total spectra. Therefore, we can conclude that for more than ≈90% of the total spectra it is required to conduct a more detailed investigation of the sky subtraction and parameters derived ("intermediate cases"). Table 2 summarizes these results.

As far as we consider the non-co-added spectra to also investigate the variability characteristic of accretors, it is worth noting that not all the bad cases have flag for each of its spectrum[11]. Tables A.1 and A.2 summarize the properties of good and bad cases, respectively.

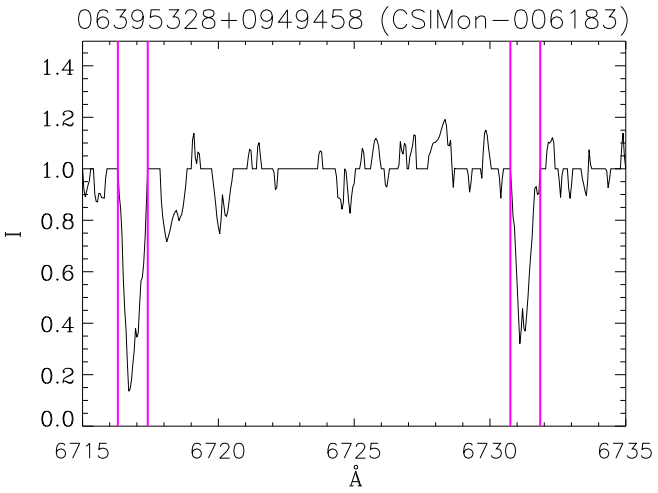

Fig. A.2. Range of the spectrum of one object around the [SII] doublet: our tool allows us to select those objects with spurious absorption features, as highlighted by the vertical magenta lines around the absorption lines in this figure.

Table A.1. Cname, spectrum used for the measurements, extremes of the [SII] doublet calculated by the tool, and FWZI for the spectra classified as "good" using our tool.

Cname	MANYSPEC.Nspec	[SII]6717min	[SII]6717max	[SII]6731min	[SII]6731max	FWZI(Hα)
06411486+0925551	C20120118-00001-st.34	6716.20	6719.20	6728.35	6733.65	14.10
06405295+0926256	C20120223-00002-st.5	6716.45	6717.25	6730.80	6731.65	14.40
06405295+0926256	C20111222-00001-st.5	6716.00	6717.35	6730.90	6731.70	14.15
06405295+0926256	C20111221-00005-st.5	6716.40	6717.20	6730.85	6731.65	14.75
06404928+0923503	C20120123-00002-st.113	6716.65	6717.00	6730.65	6731.45	14.80

Notes. Among these cases, ≈90% with Hα line in emission are defined here as "confident accretors". Caution should be used when considering the values presented in this table for parameters related to accretion process when the Hα line is in absorption – see values of Hα 10% width in the electronic version of Table 1. The complete version of this table is available at the CDS, and includes the extremes of the [NII] doublet and the object name. The FELs extremes have been derived by the sky-subtracted spectra, while the FWZI(Hα) values by the non-skysubtracted spectra. Here the information of the first five objects are reported as an example.

Table A.2. Cname, spectrum used for the measurements, extremes of the [SII] doublet calculated by the tool, and FWZI for the spectra classified as "bad" using our tool.

Cname	MANYSPEC.Nspec	[SII]6717min	[SII]6717max	[SII]6731min	[SII]6731max	FWZI(Hα)
06414719+0922535	C20111216-00001-st.44	–	–	–	–	2.30
06402778+0925193	C20120111-00001-st.118	–	–	–	–	2.35
06402492+0911195	C20121205-00012-st.102	–	–	–	–	2.95
06392623+0947066	C20121024-00039-st.115	–	–	–	–	2.60
06394446+0956006	C20121025-00049-st.121	–	–	–	–	1.45

Notes. The complete version of this table is available at the CDS, and includes the extremes of the [NII] doublet and the object name. The FELs extremes have been derived by the sky-subtracted spectra, while the FWZI(Hα) values by the non-skysubtracted spectra. Here the information of the first five objects are reported as an example. "–" indicates flagged spurious absorption features.

[10] In this case the number does not change because imposing the FWZI to be higher than 14 Å, the pure sky spectra are neglected.

[11] As an example, the object 06414719+0922535 has a flag for each [SII] and [NII] doublets only in one out of 20 spectra, but with at least one flag for one FEL in each spectrum.